AD-A041 220 AIR FORCE FLIGHT TEST CENTER EDWARDS AFB CALIF F/G 14/2
USE OF FLIGHT PATH ACCELEROMETERS IN PERFORMANCE FLIGHT TESTING--ETC(U)
1969 L H BERVEN
UNCLASSIFIED AFFTC-TIM-69-1001 NL

1 OF 1
ADA
041220

END

DATE
FILMED
7-77

FTC-TIM-69-1001

USE OF FLIGHTPATH ACCELEROMETE IN PERFORMANCE FLIGHT TESTING TEST TECHNIQUES, DATA ANALYSIS METHODS AND TYPICAL RESULTS

By
LESTER H. BERVEN
Aerospace Engineer

Air Force Flight Test Center
Edwards Air Force Base, California
Flight Test Engineering Division
Performance Engineering Branch

UNCLASSIFIED

SECURITY CLASSIFICATION OF THIS PAGE (When Data Entered)

REPORT DOCUMENTATION PAGE

READ INSTRUCTIONS BEFORE COMPLETING FORM

1. REPORT NUMBER: AFFTC-TIM-69-1001

2. GOVT ACCESSION NO.:

3. RECIPIENT'S CATALOG NUMBER:

4. TITLE (and Subtitle): Use of Flight Path Accelerometers in Performance Flight Testing: Test Techniques, Data Analysis Methods and Typical Results.

5. TYPE OF REPORT & PERIOD COVERED: Memorandum Rept. for 9 Aug 67-9 Feb 68

6. PERFORMING ORG. REPORT NUMBER:

7. AUTHOR(s): Lester H. Berven

8. CONTRACT OR GRANT NUMBER(s):

9. PERFORMING ORGANIZATION NAME AND ADDRESS: Flight Test Engineering Division/DOEE, Edwards Air Force Base CA 93523

10. PROGRAM ELEMENT, PROJECT, TASK AREA & WORK UNIT NUMBERS:

11. CONTROLLING OFFICE NAME AND ADDRESS: Same as Block 9.

12. REPORT DATE: 1969

13. NUMBER OF PAGES: 23

14. MONITORING AGENCY NAME & ADDRESS (if different from Controlling Office): Same as Block 9.

15. SECURITY CLASS. (of this report): UNCLASSIFIED

15a. DECLASSIFICATION/DOWNGRADING SCHEDULE: NA

16. DISTRIBUTION STATEMENT (of this Report)

This document has been approved for public release and resale; its distribution is unlimited.

17. DISTRIBUTION STATEMENT (of the abstract entered in Block 20, if different from Report)

18. SUPPLEMENTARY NOTES

19. KEY WORDS (Continue on reverse side if necessary and identify by block number)

A-37A Aircraft
Performance
Stability and Control
Flight Path Accelerometer (FPA)
Flight Test Techniques
Data Analysis Methods
Mach Drag Polars
External Store Drag

20. ABSTRACT (Continue on reverse side if necessary and identify by block number)

The application of flightpath accelerometers in performance flight testing has been of continuing interest to the Air Force Flight Test Center. Much practical experience in flightpath accelerometer technology was gained during performance testing the Cessna A-37A aircraft at the AFFTC. Flight test techniques used during this program were designed to take advantage of the characteristics of the FPA. The results of this testing show that the FPA can provide accurate, consistent data for defining constant Mach drag polars, external store drag, climb/

next page

DD FORM 1 JAN 73 1473 EDITION OF 1 NOV 65 IS OBSOLETE

UNCLASSIFIED

Item 19: Continued

Climb/acceleration potential
Calibration jet exhaust nozzles

Item 20: Continued

accelerate potential and can be used for in-flight calibration of jet exhaust nozzles. The accuracy and consistency of the FPA data is however, dependent on corrections for manufacturing errors, aero-dynamic upwash, errors caused by aircraft pitch rates and accelerations and for the response lag of the FPA/vane unit during rapid angle of attack changes. This report explains some of the problems encountered while using the FPA and the corrections which were devised to solve them. It explains the data analysis methods used and presents flight test data for the maneuvers described.

When US Government drawings, specifications, or other data are used for any purpose other than a definitely related government procurement operation, the government thereby incurs no responsibility nor any obligation whatsoever; and the fact that the government may have formulated, furnished, or in any way supplied the said drawings, specifications, or other data is not to be regarded by implication or otherwise, as in any manner licensing the holder or any other person or corporation, or conveying any rights or permission to manufacture, use, or sell any patented invention that may in any way be related thereto.

Do not return this copy. Retain or destroy.

AFSC-EDWARDS AFB, MUROC CAL

USE OF FLIGHTPATH ACCELEROMETERS IN PERFORMANCE FLIGHT TESTING: TEST TECHNIQUES, DATA ANALYSIS METHODS AND TYPICAL RESULTS

By

LESTER H. BERVEN
Aerospace Engineer

AIR FORCE FLIGHT TEST CENTER
EDWARDS AIR FORCE BASE, CALIFORNIA
FLIGHT TEST ENGINEERING DIVISION
PERFORMANCE ENGINEERING BRANCH

FOREWORD

This memorandum is a summary of the practical experience gained in using a dual-axis flightpath accelerometer during the A-37A Category II performance testing conducted at the Air Force Flight Test Center, Edwards Air Force Base, California, between 9 August 1967 and 9 February 1968.

This memorandum was prepared by:

LESTER H. BERVEN
Project Engineer

Approved by:

CROWELL B. WERNER, Colonel, USAF
Chief Flight Test Engineering Division

ABSTRACT

The application of flightpath accelerometers in performance flight testing has been of continuing interest to the Air Force Flight Test Center. Much practical experience in flightpath accelerometer technology was gained during performance testing of the Cessna A-37A aircraft at the AFFTC. Flight test techniques used during this program were designed to take advantage of the characteristics of the FPA. The results of this testing show that the FPA can provide accurate, consistent data for defining constant Mach drag polars, external store drag, climb/acceleration potential and can be used for in-flight calibration of jet exhaust nozzles. The accuracy and consistency of the FPA data is, however, dependent on corrections for manufacturing errors, aerodynamic upwash, errors caused by aircraft pitch rates and accelerations and for the response lag of the FPA/vane unit during rapid angle of attack changes. This report explains some of the problems encountered while using the FPA and the corrections which were devised to solve them. It explains the data analysis methods used and presents flight test data for the maneuvers described.

SYMBOLS AND ABBREVIATIONS

Item	Definition	Units
A	acceleration potential	ft per sec^2
A_f	acceleration factor	dimensionless
AFFTC	Air Force Flight Test Center	---
A_8	engine exhaust nozzle area	ft^2
C_D	airplane total drag coefficient	dimensionless
C_g	gross thrust coefficient	dimensionless
C_L	airplane lift coefficient	dimensionless
D	drag	lb
f	frequency	cycles per second
F_e	engine ram drag	lb
F_{ex}	excess thrust	lb
F_g	gross thrust	lb
f_n	natural frequency	cycles per second
F_N	net thrust component along the flightpath	lb
FPA	flightpath accelerometer	---
g	acceleration due to gravity	32.17405 ft per sec^2
h	altitude	ft
KEAS	knots equivalent airspeed	---
KIAS	knots indicated airspeed	---
ℓ_v	distance from the FPA unit to the aircraft center of gravity	ft
N_x	true load factor along the flightpath	dimensionless
N_{x_m}	measured load factor along the flightpath	dimensionless
N_z	true load factor perpendicular to the flightpath	dimensionless

Item	Definition	Units
N_{z_m}	measured load factor perpendicular to the flightpath	dimensionless
P_a	ambient pressure	in.Hg
P_{t_8}	engine exhaust nozzle total pressure	in.Hg
r	damping ratio	dimensionless
R/C	rate of climb	ft per min
S/N	serial number	---
USAF	United States Air Force	---
V_t	true airspeed	kt
W	airplane gross weight	lb
α	angle of attack	deg
$\Delta\alpha$	angle of attack increment	deg
δ_a	ambient pressure ratio	dimensionless
ϵ	vane misalignment angle due to a combination of mechanical misalignment, upwash, pitch rate and response lag	deg
$\dot{\theta}$	pitch rate about the aircraft center of gravity	rad per sec
$\ddot{\theta}$	pitch acceleration about the aircraft center of gravity	rad per sec^2
γ	flightpath angle	deg
Ψ	reference angle	deg
Ψ_g	nozzle pressure ratio parameter	dimensionless
ϕ	phase angle	deg

USE OF FLIGHTPATH ACCELEROMETERS IN PERFORMANCE FLIGHT TESTING: TEST TECHNIQUES, DATA ANALYSIS METHODS AND TYPICAL RESULTS

INTRODUCTION

The application of flightpath accelerometers in performance flight testing has been an item of continuing interest to the Air Force Flight Test Center (AFFTC). Although some reports have been written on this subject they have generally tended toward a detailed description of the operation of the flightpath accelerometer, with a few suggested applications.

The information contained in this report is a result of the practical experience obtained during the A-37A performance and stability and control flight testing at the AFFTC. It includes the flight test techniques used during this program to take advantage of the characteristics of the flightpath accelerometer (FPA); it explains some of the unique problems which were encountered and the corrections devised to solve them. It also explains the data analysis methods used and presents flight test data for the maneuvers described.

DESCRIPTION OF TEST INSTRUMENTATION

The dual axis flightpath accelerometer (FPA) used during the A-37A testing was a Systron-Donner Model 4310. This accelerometer unit was mounted inside a 3-inch diameter test boom which extended 8 feet in front of the aircraft nose. The sensitive axes of the FPA were aligned with the relative wind (and therefore the flightpath) by a 16-degree wedge vane located on the side of the boom. The vane pivoted coaxially with the

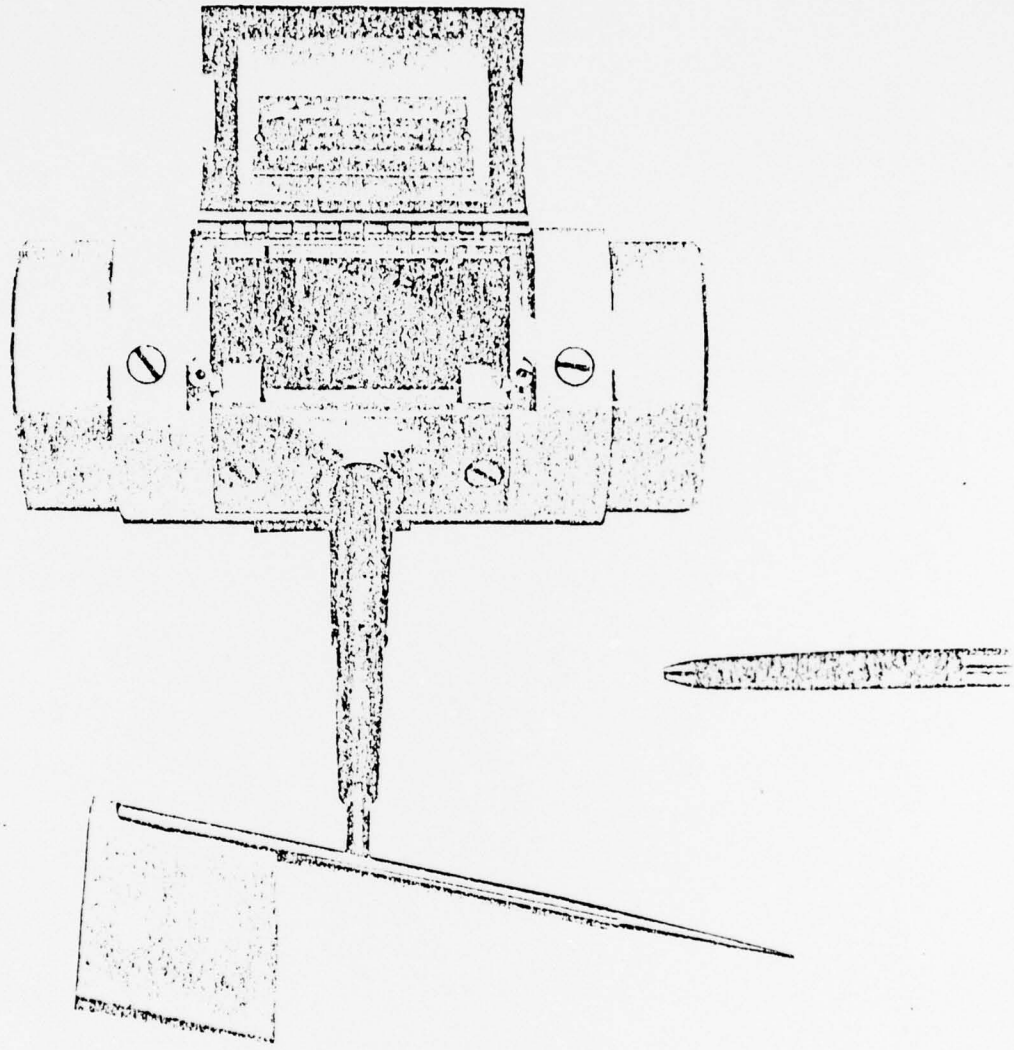

Figure 1. FPA/VANE UNIT

FPA. The FPA/vane unit was free to move through an angle of ±30 degrees with respect to the boom (see figure 1). The FPA output (a voltage proportional to acceleration) was read out on an oscillograph using a Vernier range extender. The range extender effectively increased the equivalent trace deflection to ±30 inches for ±0.5 g (longitudinal) and ±8 g (normal). Pre- and postflight zeros were obtained by aligning the longitudinal and normal sensitive axes parallel and perpendicular, respectively, to local gravity. This was done by attaching a pendulum to the vane and swinging it to obtain a gravity level. Another swing was made with the pendulum reversed to average its mechanical misalignment.

APPLICATIONS AND TEST TECHNIQUES

The use of the FPA in performance flight testing is based on the relation:

$$\text{Drag} = F_N - F_{ex}$$

where $F_{ex} = (F_N - D) = N_x \cdot W$

The accurate in-flight measurement of N_x permits the calculation of drag during nonsteady state maneuvers, thereby reducing significantly the test time required to obtain drag data.

The following paragraphs describe some of the applications of this principle and some of the test techniques devised to take advantage of the characteristics of the FPA.

Constant Mach Drag Polars

To obtain lift/drag data at constant Mach number, two maneuvers were used——roller coasters and windup turns.

Roller coasters were started from trimmed level flight at the desired Mach number and altitude. The pilot then varied load factor cyclically from +2 to 0 g's by longitudinal stick inputs. The resulting changes in induced drag were reflected by corresponding deceleration and acceleration readings from the FPA. The combined normal and longitudinal accelerometer values yielded the shape and slope of the drag polar at the trim Mach number through the following equations:

$$C_L = \frac{0.000675\ (N_Z W - Fg \sin \alpha)}{\delta_a\ M^2\ S} \qquad (1)$$

$$C_D = \frac{0.000675\ (Fg \cos \alpha - F_e - N_X W)}{\delta_a\ M^2\ S} \qquad (2)$$

Airspeed changes were generally inversely proportional to the frequency of the maneuver (cyclic change of load factor), and at low maneuver frequencies (approximately 1/10 cycles/second) the airspeed changes were significant enough to require Mach corrections to the drag data. At maneuver frequencies greater than 1/5 cycles/second, FPA/vane response errors resulted in a hysteresis band in the drag polar. Roller coasters were therefore limited to relatively small load factor excursions because of these two limitations.

Windup turns were used to obtain the same information provided by the roller coasters but at higher load factors. These maneuvers were also started from trimmed level flight at the desired Mach number but were begun 500 feet above the aim altitude. Once the trim data was obtained, the aircraft was nosed down to increase airspeed approximately 10 to 20 KIAS above trim speed. The nose was then pulled up above the horizon, and as airspeed decreased to trim Mach number a pushover was made to zero g. As Mach number approached the trim value, the aircraft was rolled into a turn and back stick was added to

increase load factor. Mach number was maintained constant by increasing rate of descent as load factor was increased. The induced drag increase with g loading was just offset by the increase in effective thrust resulting from the rate of descent. In this manner drag data could be obtained at approximately constant Mach number up to either the limit load factor of the aircraft or stall, whichever occurred first. For a typical 4-g windup turn, altitude loss was 500 feet.

Both the roller coaster and windup turn data showed the slope of the A-37A drag polars to be essentially constant, even at higher Mach numbers, and yielded lines parallel to the low Mach polar but displaced as a function of the drag rise due to compressibility. For the same Mach number and C_L range, the two methods gave identical drag polars.

Examples of roller coaster and windup turn data are shown in figures 2 and 3, with a speed power drag polar fairing included for comparison.

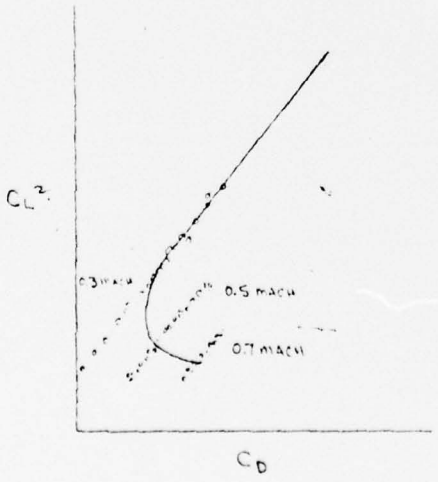

Figure 2. Roller Coasters

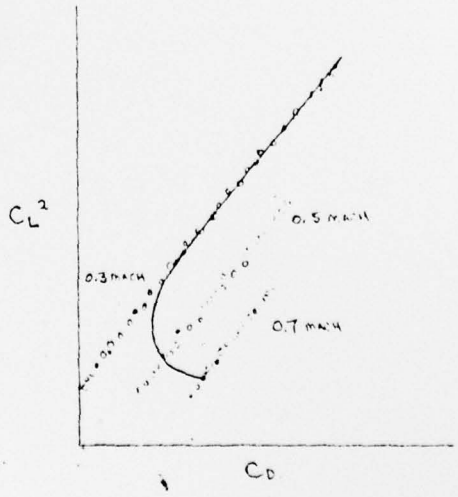

Figure 3. Windup Turns

Incremental External Store Drag

The drag of several types of external stores was determined by analyzing the flightpath acceleration which resulted from dropping a pair of stores, one each from symmetrically opposite wing pylons.

The store drag increment was determined from a C_L^2 versus C_D plot as shown in figure 4. The points to the right are the trim points and the points to the left are a short time history of C_L^2 versus C_D after the drop. The slope of the fairings through the points was determined from a roller coaster performed at trim conditions. Drops could be made at several airspeeds and altitudes to determine the variation of store drag with Mach number.

Another method investigated was to perform roller coasters before and after the drop, restabilizing at the same Mach number and altitude. However, this technique required that engine thrust be changed to compensate for the drag change and therefore was dependent on absolute in-flight thrust values for the incremental drag. With the stabilized drop method, the accuracy of the total drag data was still limited to the accuracy of the thrust values used; however, the incremental store drag depended only upon the accuracy of the resulting flightpath acceleration and the aircraft weight. Data were obtained by both methods, but the incremental values obtained by the stabilized drop method were consistently more repeatable. Reference 1 contains the results of these tests for 9 typical stores.

Climb/Acceleration Potential

The flightpath accelerometer provided a rapid, accurate means of determining the climb/acceleration potential of the aircraft from maximum power level accelerations. Consider the following simplified analysis.

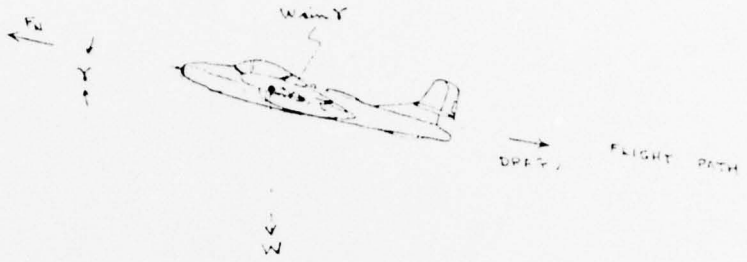

Setting a summation of forces along the flightpath equal to mass times acceleration along the flightpath gives:

$$(F_N - D - W \sin \gamma) = \frac{W}{g} \frac{dV_t}{dt}$$

or $$F_{ex} = (F_N - D) = (W \sin \gamma + \frac{W}{g} \frac{dV_t}{dt})$$

$$F_{ex} = W (\sin \gamma + \frac{dV_t/dt}{g}) \quad (3)$$

When the longitudinal accelerometer is tilted from the horizontal in the absence of any external acceleration, its output is the sine of the tilt angle. In a climb, the accelerometer is at an angle from the horizontal equal to the climb angle γ, so the output is sin γ. Any additional acceleration along the flightpath (dV/dt) is sensed as a linear addition to the first value. Therefore, the output of the longitudinal FPA is:

$$N_x = (\sin \gamma + \frac{dV_t/dt}{g}) \quad (4)$$

The longitudinal FPA reading times the aircraft weight at any flight condition, then, is equal to the excess thrust, or

$$F_{ex} = N_x \cdot W \tag{5}$$

also, $$\sin \gamma = \frac{dh/dt}{V_t}$$

$$\frac{dV_t}{dt} = \frac{dh}{dt} \cdot \frac{dV_t}{dh}$$

substituting in equation (3),

$$F_{ex} = W \left(\frac{dh/dt}{V_t} + \frac{dh/dt}{g} \cdot \frac{dV_t}{dh} \right) \tag{6}$$

solving for dh/dt = R/C,

$$R/C = \frac{F_{ex}\ V_t}{\left[1 + \frac{V_t}{g} \frac{dV_t}{dh}\right] W} \tag{7}$$

defining $\left(1 + \frac{V_t}{g} \frac{dV_t}{dh}\right)$ as the acceleration factor A_f (the correction to R/C for an acceleration $\frac{dV}{dh} \cdot \frac{dh}{dt}$),

$$R/C = \frac{F_{ex} \cdot V_t}{A_f \cdot W} \tag{8}$$

and from equation (3) with no climb rate ($\gamma = 0$), the aircraft acceleration potential is:

$$A = \frac{F_{ex} \cdot g}{W} \tag{9}$$

A plot of F_{ex}/W versus Mach and altitude can be developed by conducting military power level flight accelerations at various altitudes and loadings. (Reference 2 gives methods for correcting test excess thrust to standard conditions.) With this plot, any combination of climb rate and/or acceleration for a given weight can easily be determined.

In-Flight Thrust Calibration

It is a well known fact that static thrust runs conducted at low altitudes do not calibrate the engine exhaust nozzle for all values of nozzle pressure ratio, P_{t8}/P_a, attainable in flight. In fact, the maximum static value of P_{t8}/P_a is usually far short of that attainable at high altitudes and high Mach numbers. The flightpath accelerometer provides a means of extending the ground static thrust run to cover in-flight values of P_{t8}/P_a in the following manner.

Given the results of the ground thrust run, presented as gross thrust coefficient C_g versus P_{t8}/P_a:

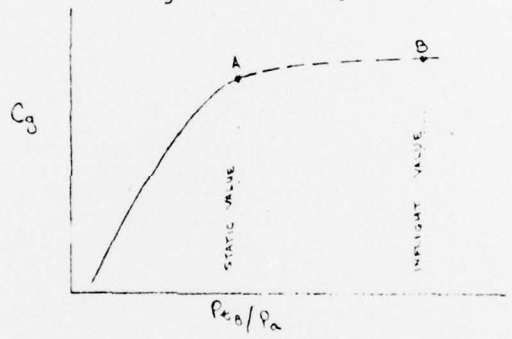

and $F_g = C_g \Psi_g P_a A_8$

If two level accelerations are performed through the same speed V_t, using power settings A and B, two different values of N_x will be obtained. The excess thrust at points A and B is:

$$F_{ex_A} = N_{x_A} \cdot W_A \tag{10}$$

$$F_{ex_B} = N_{x_B} \cdot W_B \tag{11}$$

and $(F_{ex_B} - F_{ex_A})$ is the change in net thrust between points A and B. Therefore, $F_{N_B} = F_{N_A} + (F_{ex_B} - F_{ex_A})$ (12)

Since the ram drag at each point can be calculated, the second

gross thrust is also available, and

$$F_{g_B} = F_{N_B} + F_{e_B} \tag{13}$$

$$C_{g_B} = \frac{F_{g_B}}{(\Psi\ A_8\ P_a)_B}$$

A series of these accelerations can be conducted to extend the line in figure 6 to the desired value of P_{t_8}/P_a. More detailed corrections for changes in induced drag and angle of attack are included in reference 3.

DATA ANALYSIS METHODS

It has been assumed in all of the discussions in this report that an accurate value of N_x and N_z were available for data reduction. For this to be true, however, several corrections have to be made to the N_x and N_z outputs read from the oscillograph. The corrections required during the A-37A program were:

1. For misalignment of the vane and accelerometer sensitive axes.

2. For misalignment of the vane and flightpath due to aerodynamic upwash.

3. For upflow at the vane caused by aircraft pitch rate.

4. For inertial errors caused by aircraft pitch rates and accelerations.

5. For the response lag of the FPA/vane unit during rapid angle of attack changes.

The following paragraphs describe how these errors affect the final data and how the recommended corrections are applied.

Mechanical FPA/Vane Misalignment

A misalignment of the FPA sensitive axis and the vane results in a constant error in N_x and N_z. The magnitude of this error can be determined from the pre- and postflight pendulum swings described previously. The average of the longitudinal accelerometer output with the pendulum mounted normally, and with it reversed, is the vane level N_x output. If this value is different from zero, its magnitude is equal to the mechanical misalignment angle in radians. The value of this angle for the A-37A FPA/vane unit was 0.6 degrees, or 0.0105 radians. This error is considerable, since for a 10,000-pound airplane at one g, it results in a constant excess thrust reading of 105 pounds. This error is increased in proportion to normal load factor.

Aerodynamic Upwash

During stabilized speed power tests it was found that the longitudinal accelerometer (corrected for mechanical misalignment) indicated some value of acceleration, even though an airspeed time history showed dV/dt to be zero. This error was repeatable and systematic and was a unique function of lift coefficient. Aircraft configuration or store loading had no apparent effect. These erroneous N_x values were finally attributed to aerodynamic upwash caused by the fuselage, wings and noseboom. The values for upwash effects given in reference 4 and calculated from reference 5 show the same shape curve as the flight test data. The upwash data obtained from the speed power tests is shown in figure 5.

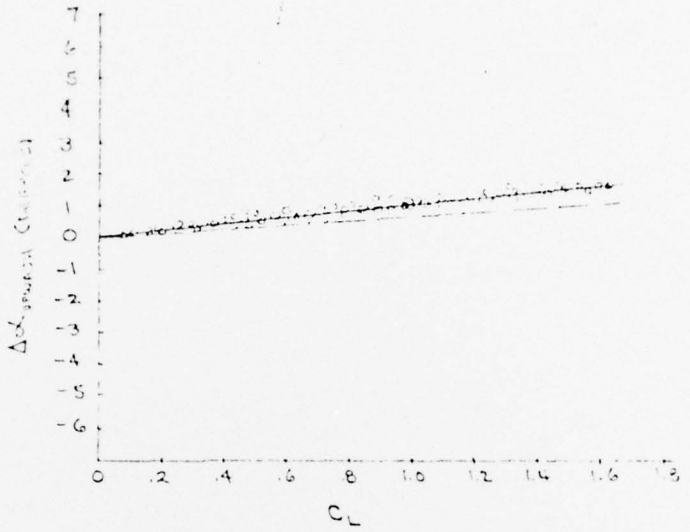

Figure 5. Accelerometer Upwash Error

These data were obtained by assuming stabilized flight and taking the corrected value of N_X as the arcsin of the upwash angle. Any angle of the vane with respect to the horizontal causes the longitudinal FPA to read a component of acceleration due to gravity. The fairing shown in figure 5 was used to correct all FPA data for upwash as a function of lift coefficient. The dashed line is the theoretical value from references 4 and 5. Note that in some cases this error was as large as or larger than that caused by mechanical misalignment.

Pitch Rate and Pitch Acceleration

During the roller coaster and windup turn maneuvers, accelerometer errors were induced by the pitch rate and pitch acceleration of the aircraft.

The errors due to pitch rate were twofold. The first was a misalignment of the vane from the flightpath resulting from the vertical velocity component at the vane. The magnitude of this misalignment due to pitch rate was calculated from the following equation:

$$\epsilon_{PR} = \tan^{-1} \left(\frac{\ell_V \cdot \dot{\theta} \cdot \cos \alpha}{V_t} \right) \qquad (15)$$

The second factor was the centrifugal force effect on the accelerometers. This error was proportional to the vane length from the cg of the aircraft and the square of the pitch rate.

Additional errors were caused by tangential accelerations at the FPA resulting from the pitch accelerations of the aircraft.

All of these errors and the errors caused by mechanical misalignment and upwash, were corrected using the following equations:

$$N_Z = N_{Z_m} \cos \epsilon + N_{X_m} \sin \epsilon + \frac{\ell_V \dot{\theta}^2}{g} \sin \alpha - \frac{\ell_V \ddot{\theta}}{g} \cos \alpha \qquad (16)$$

$$N_X = N_{X_m} \cos \epsilon - N_{Z_m} \sin \epsilon + \frac{\ell_V \dot{\theta}^2}{g} \cos \alpha + \frac{\ell_V \ddot{\theta}}{g} \sin \alpha \qquad (17)$$

where:

N_Z, N_X = corrected values of normal and longitudinal flightpath acceleration

N_{Z_m}, N_{X_m} = indicated values of normal and longitudinal flightpath acceleration

ϵ = misalignment angle due to a combination of mechanical misalignment, upwash and pitch rate

ℓ_V = distance from the FPA to the cg of the aircraft in feet

$\dot{\theta}$ = pitch rate in rad/sec about the aircraft cg

$\ddot{\theta}$ = pitch acceleration in rad/sec^2 about the aircraft cg

α = noseboom reference line angle of attack

Derivation of these correction equations and terms to include yaw and roll rates are given in reference 6.

FPA Vane Response

As was mentioned previously, roller coaster data showed a hysteresis band in the resulting drag polar. The width of the hysteresis band was proportional to both the amplitude (angle of attack excursion) and frequency of the maneuver. A typical high frequency roller coaster (1/3 cycles/sec) with all the previously described corrections made is shown in figure 6.

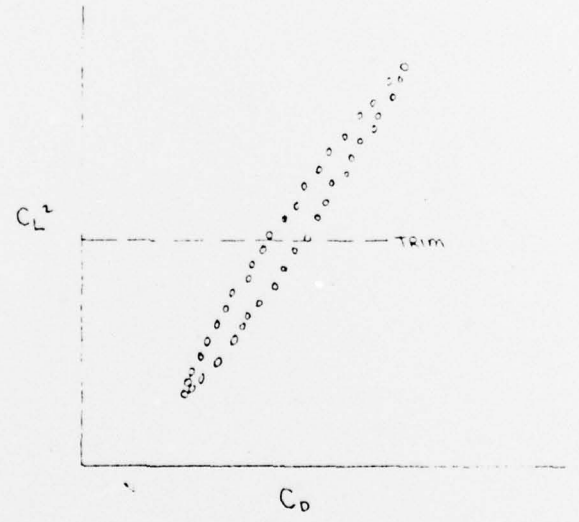

Figure 6. Roller Coaster with Response Error

The hysteresis band here is quite evident and indicates that an additional correction is required for high frequency roller coaster data.

The accelerometer, vane, bearing and airflow combination can be considered a linear second order system. The spring constant is the aerodynamic restoring torque, proportional to vane angle of attack; the damping term is a combination of bearing friction and aerodynamic damping, and the inertial term is the rotational moment of inertia of the accelerometer/vane/shaft combination.

A perfect vane would maintain a zero angle of attack at all times, thereby following the forcing function exactly; however, for an actual linear second order system there is a finite phase lag between the forcing function and the system response. This phase lag is a function of the damping ratio of the second order system and the ratio of the forcing frequency to the system natural frequency. Tests conducted on this type FPA/vane unit indicate a resonant frequency between 10 and 15 cps and a damping ratio of approximately 0.2 to 0.4. Typical second order phase response curves are shown in figure 7.

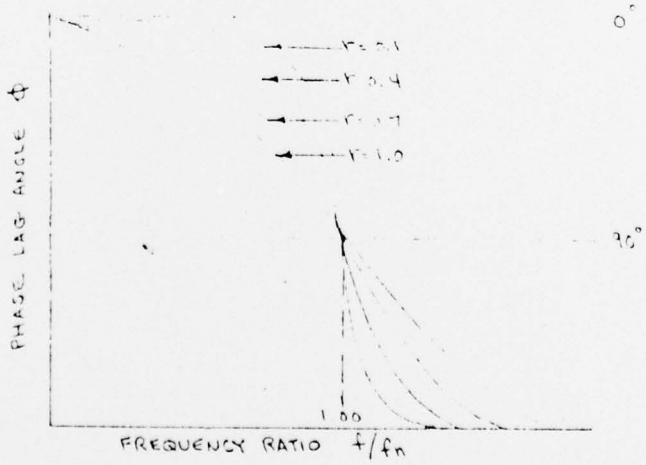

Figure 7 Second Order Response

For a maneuver frequency = 0.5 cps, assume f_n = 12 cps and r = 0.3; f/f_n therefore = .04, and ϕ = 2 degrees.

If a sinusoidal variation in angle of attack is assumed (and test data indicate that this is a reasonable assumption),

$$\alpha_{true} = \alpha_{max} \sin \Psi$$

where Ψ is the reference angle along the sine wave of α versus time.

With a phase lag angle ϕ,

$$\alpha_{indicated} = \alpha_{max} \sin (\Psi - \phi)$$

The vane lag angle ϵ is then

$$\epsilon = \alpha_{true} - \alpha_{indicated}$$

$$\epsilon = \alpha_{max} [\sin \Psi - \sin (\Psi - \phi)]$$

assuming cos ϕ = 1.0 and substituting

$$\sin (\Psi - \phi) = (\sin \Psi \cos \phi - \cos \Psi \sin \phi)$$

$$\epsilon = \alpha_{max} (\cos \Psi \sin \phi)$$

The phase angle ϵ calculated from this equation can then be used with equations 16 and 17 to obtain corrected values of N_X and N_Z. Since the natural frequency and damping ratio of the A-37A FPA unit was unknown, phase angle ϕ was varied in an iteration procedure until minimum hysteresis was obtained. The roller coaster data shown in figure 6 was corrected in this manner, the results are shown in figure 8. Some of the remaining

scatter can be attributed to a nonsinusoidal variation in angle of attack during the maneuver or to the fact that the FPA/vane unit response was not entirely linear second order.

CONCLUSIONS

The use of flightpath accelerometers in performance flight testing provides a rapid, accurate method of obtaining data for constant Mach drag polars, external stores drag and energy/maneuverability plots, and has a potential use in calibrating jet engine exhaust nozzles in flight. Several corrections to the flightpath accelerometer output are required to obtain accurate values of acceleration along the flightpath.

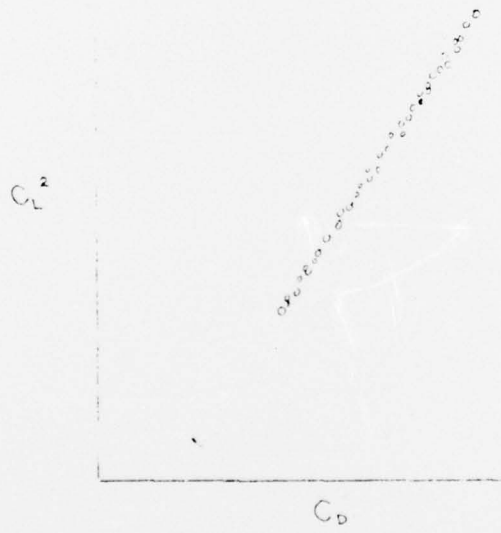

Figure 8. Roller Coaster Corrected for Response Error

REFERENCES

1. Lester H. Berven, Roger J. Smith, Captain, USAF, A-37A Category II Performance Tests, FTC-TR-68-23, Air Force Flight Test Center, January 1969.

2. Richard C. Walker, Captain, USAF, Determination of an Aircraft's Standard Climb and Level Acceleration Performance, FTC-TR-64-40, Air Force Flight Test Center, May 1965.

3. Willie L. Allen, "Proposed Techniques for In-flight Calibration of Jet Engine Exhaust Nozzles," (Unpublished Technical Information Memorandum, Air Force Flight Test Center, April, 1967).

4. D. E. Beeler, R. Bellman, E. J. Saltzman, Flight Test Techniques for Determining Airplane Drag at High Mach Numbers, NACA TN 3821, 1956.

5. The Dornier Company (GMBH), Friedrichshafen/Bodensee, West Germany, Report on Flight Test Measuring Equipment, Translated by Volker M. Storch, November 1967.

6. Milton B. Porter, Jr., Captain, USAF, Boom Mounted Accelerometer and Angle of Attack Vane Errors Induced by Body Angular Rates and Accelerations, Flight Research Branch Office Memo, Air Force Flight Test Center, April 1967.

A-37A USAF S/N 67-14507
J85-GE-17A Engines
Cruise Configuration

Gross Weight Before Drop	9300	lb	Airspeed	220	KEAS
Weight of Stores Dropped	1390	lb	Altitude	10,000	ft
Flight Number 64	Run Number 8		Mach Number	.40	

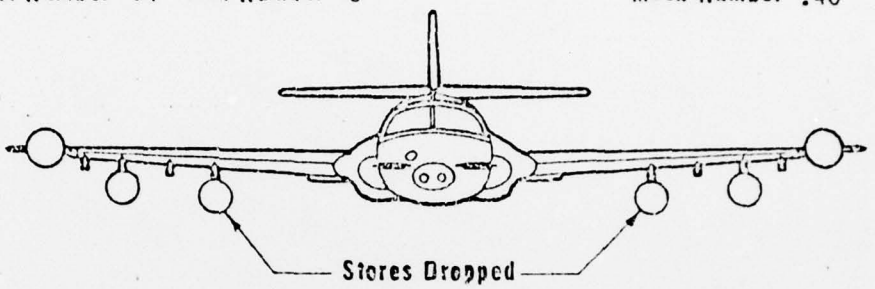

Pylons	Stores
LR1	BLU1/CB
LR3	LAU32A

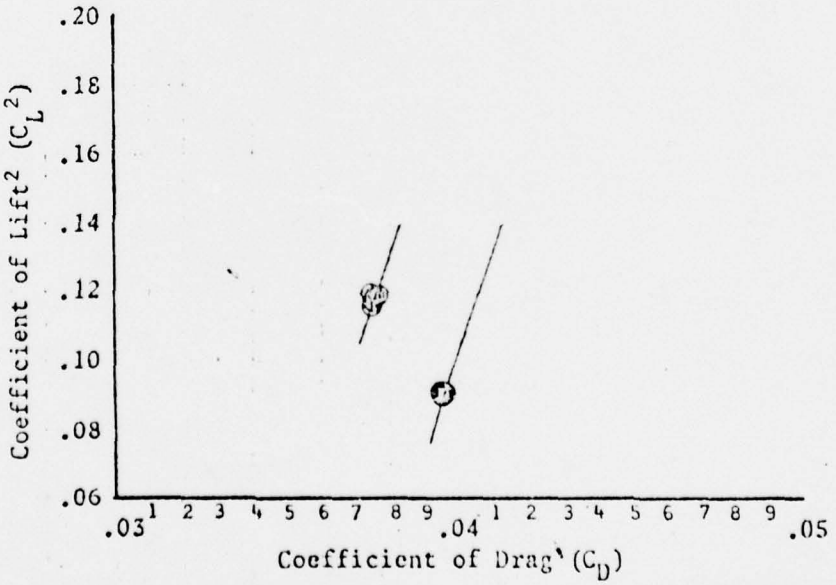

Figure 1 EXTERNAL STORE DRAG